CIRSE

Comparison of Tc-99m MAA Planar Versus SPECT/CT Imaging for Lung Shunt Fraction Evaluation Prior to Y-90 Radioembolization: Are We Overestimating Lung Shunt Fraction?

Mohammad Elsayed[1] · Bernard Cheng[2] · Minzhi Xing[1] · Ila Sethi[3] ·
David Brandon[3] · David M. Schuster[3] · Zachary Bercu[1] · James Galt[3] ·
Bruce Barron[3] · Nima Kokabi[1]

Abstract

Purpose To compare lung shunt fraction (LSF) prior to Y-90 radioembolization calculated using planar imaging versus SPECT/CT in patients with hepatocellular carcinoma (HCC).

Methods A single institution retrospective analysis of technetium-99m macroaggregated albumin (Tc-99m MAA) LSF studies for 293 consecutive patients with HCC between 2013 and 2018 was performed. LSF using planar imaging (PLSF) was compared to retrospectively calculated LSF using SPECT/CT (SLSF) via semiautomated segmentation using MIM v.6.9. Sub-analyses of patients were performed based on PLSF range, tumor size, BCLC stage, and Child–Pugh (C–P) score. Mean LSF absolute discrepancy between sub-groups was analyzed. Comparisons were performed using paired t tests and linear regression analysis.

Results Mean PLSF, 8.27%, was greater than mean SLSF, 3.27% ($p < 0.001$). When categorizing patients by PLSF ranges of < 10%, 10–19.9%, and ≥ 20%, PLSF remained greater than SLSF in all subgroups (p's < 0.001). Patients with PLSF ≥ 20% had a greater absolute discrepancy with SLSF (13.31%) compared to patients with PLSF < 20%

(4.74%; $p < 0.0001$). LSF absolute discrepancy was greater for patients with a maximum liver tumor size ≥ 5.0 cm (5.59%) compared to a liver tumor size < 5.0 cm (4.40%; $p = 0.0076$). For all BCLC grades and C–P scores, PLSF was greater than SLSF. A greater LSF discrepancy existed for patients with a worse C–P score (C–P A: 4.78%, C–P B/C: 6.12%; $p = 0.0081$), but not BCLC stage (0/A/B: 4.87%, C: 4.56%; $p = 0.5993$).

Conclusion In patients with HCC, SLSF is significantly lower compared to PLSF, with a greater discrepancy among patients with a PLSF ≥ 20%, tumor size ≥ 5 cm, and worse C–P score.

Level of Evidence Level 3, Retrospective Study.

✉ Mohammad Elsayed
mohammad.elsayed@emory.edu

1 Division of Interventional Radiology and Image-Guided Medicine, Department of Radiology and Imaging Sciences, Emory University School of Medicine, 1364 Clifton Road NE, Suite BG03, Atlanta, GA 30322, USA

2 Morehouse School of Medicine, Atlanta, GA, USA

3 Division of Nuclear Medicine and Molecular Imaging, Department of Radiology and Imaging Sciences, Emory University, Atlanta, GA, USA

Introduction

Yttrium-90 (Y-90) radioembolization (RE) is a procedure performed in patients with hepatic malignancies in which radiolabeled Y-90 microspheres are injected into a hepatic artery feeding tumor [1]. In carefully selected patients with unresectable hepatocellular carcinoma (HCC), Y-90 radioembolization improves tumor response and overall survival compared to conventional therapies [2–5].

Before Y-90 RE, angiographic mapping is performed to evaluate hepatic vasculature and the risk of non-target embolization [1]. During this procedure, technetium-99m macroaggregated albumin (Tc-99m MAA) is administered into the hepatic arteries in order to, in addition to other uses, evaluate lung shunt fraction (LSF). LSF from Tc-99m MAA is typically estimated with planar imaging, in which

a geometric mean is calculated using counts of the liver and lungs from anterior and posterior views [6, 7]. Multiple studies indicate that planar imaging is limited by inaccurate organ segmentation and scatter artifact [6, 8, 9]. This may result in overestimation of LSF, particularly from lesions near the hepatic dome, which may be erroneously localized to the lungs instead of the liver [7].

Growing evidence suggests that a major contributor to incomplete treatment response after Y-90 RE is due to insufficient dose delivered to target tumors [10–13]. Due to the potentially inaccurate LSF calculated by planar imaging, Y-90 dose may be sub-optimally adjusted resulting in under-treatment of patients. In addition, certain patients with elevated LSF based on planar imaging may be considered ineligible for Y-90 RE due to concerns for radiation-induced pneumonitis and established dose limits to the lungs [14]. This necessitates the need for more accurate assessment of hepatopulmonary shunting and Y-90 dose calculation.

SPECT/CT has been proposed as an alternative method to estimating LSF [15, 16]. When used in conjunction with semiautomated segmentation software, SPECT/CT is likely advantageous in adjusting for artifacts and accurately delineating liver and lung parenchyma. The purpose of this study is to compare the difference of LSF using planar imaging (PLSF) versus retrospectively calculated LSF using SPECT/CT (SLSF) in patients with HCC.

Materials and Methods

Study Selection

This study has been approved by the local Institutional Review Board, and the need for written informed consent was waived. A retrospective analysis of all patients with hepatocellular carcinoma who underwent planar Tc-99m MAA LSF imaging between January 2013 and March 2018 was performed. All patients were referred to interventional radiology for Y-90 RE through multidisciplinary tumor boards. Data were collected from two large university-affiliated tertiary care hospitals in a single institution. All patients who had Y-90 planning procedures underwent concurrent imaging with SPECT/CT from the thorax to mid-abdomen, permitting SLSF evaluation. The exclusion criteria included patients who had SPECT/CT imaging which did not sufficiently include the lung parenchyma (usually the upper thorax) within the field of view.

Patients selected for Y-90 at the authors' institution met the following criteria: LSF calculated on planar images where calculated administered activity to achieve 120 Gy to target lobe resulted in estimated lung dose < 30 Gy, tumor burden < 75% of whole liver, absence of uncorrectable gastrointestinal flow on diagnostic angiogram, serum albumin > 2.5 g/dL, serum bilirubin < 2 mg/dL, and aspartate aminotransferase/alanine aminotransferase < 5 times normal upper limit.

Lung Shunt Fraction Evaluation

All patients selected for Y-90 RE underwent routine preprocedural angiography and administration of Tc-99m MAA into the hepatic artery vasculature for evaluation of hepatopulmonary shunting. Procedures were performed as described in previous literature [1]. Briefly, prior to Tc-99m MAA administration, angiography was performed for procedural planning and embolization was performed in branch vessels thought to be at high risk for non-target embolization. Cone beam computer tomography (CBCT) was then performed to ensure perfusion of the entire tumor(s). If the entire tumor(s) were not perfused from the microcatheter location, either the microcatheter location was adjusted and the process was repeated or MAA was injected in a split dose to ensure the entire treatment lobe or segment was covered. Approximately, 148 MBq (4 mCi) of Tc-99m MAA (Jubilant Pharma Holdings, Yardley, Pennsylvania, USA) were administered in total. Within 1 h after administration, planar images of patients' lung and liver area were acquired. SPECT/CT was subsequently performed for radiotracer localization and determination of possible extra-hepatic and extra-pulmonary activity. SPECT/CT images centered at the level of the liver were acquired on a Siemens Symbia T6 dual-head SPECT/CT scanner (Siemens Healthcare, Erlangen, Germany) using 140 keV, 15% energy window, 30 stops at 22 s per stop for 60 projections. SPECT reconstruction used the manufacturer's ordered subset expectation maximization-based software (6 subsets, 16 iterations) with CT-based attenuation correction and scatter correction.

To calculate PLSF, 5 min static anterior and posterior acquisitions of the chest and upper abdomen were acquired with a gamma camera using a low-energy high-resolution parallel collimator, as described in the prior literature [1]. Region of interest (ROI) boxes were drawn manually over the liver and individual lung fields. Using counts from the ROIs, PLSF was obtained by calculating the geometric mean of photon counts. SLSF was evaluated utilizing attenuation-corrected SPECT/CT images of the liver and lungs. Semiautomated segmentation of the liver and lung parenchyma was performed with MIM v6.9 software (MIM Software, Columbus, OH, USA). Automated segmentation of the liver and lungs was performed by creating volumetric analysis using axial images and multiplanar reformats. Subsequently, segmentation of the liver and lungs were manually modified to ensure that the target organs were correctly outlined. This was performed on multiple

planes. The most common modification performed was ensuring the hepatic dome (and tumors) were appropriately segmented as liver, rather than lung base which occurred due to motion artifact and misregistration (Fig. 1).

Statistical Analysis

All included patients were evaluated for age, PLSF, largest liver lesion size, Barcelona Clinic Liver Cancer (BCLC) stage, and Child–Pugh (C–P) score. Retrospective calculations of SLSF were performed. Mean SLSF was compared to mean PLSF between groups. Multiple subgroup comparisons were performed, including patients grouped by a PLSF range of < 10%, 10–19.9%, and ≥ 20%; largest liver tumor size of < 5.0 cm, 5–10 cm, and ≥ 10 cm; BCLC stage; and C–P score. Absolute discrepancy, defined as the difference between the percent of PLSF and SLSF, was calculated. Absolute discrepancy was compared between patients grouped by a PLSF of < 20 versus ≥ 20%, BCLC stage of 0, A, or B versus C, and C–P score of A versus B. Comparisons were performed using paired t tests, with a p value below 0.05 defined as statistically significant. Multiple linear regression models were used to analyze the effect of covarites and interactions between covariates on the discrepancy between PLSF and SLSF.

Statistical analysis was performed using Microsoft Excel (Microsoft Corporation, Redmond, Washington, USA), Graphpad Prism 8 (GraphPad Software, San Diego, California, USA), and SAS version 9.4 (SAS Institute, Cary, North Carolina, USA).

Results

There were a total of 298 patients identified, with 293 patients ultimately included in the analysis. Five patients were excluded from the analysis due to incomplete acquisition of the upper thorax. The study group had a mean age of 64.5 years and was 78.8% male (SD 9.71; Table 1). Of patients with known BCLC stage, there were nine patients with a stage 0, 95 patients with stage A, 80 patients with stage B, 34 with stage C, and 0 with stage D. BCLC stage was not documented and could not be retrospectively assessed in the remaining 77 patients. PLSF was greater than SLSF in 283 of 293 studies, equivalent to SLSF in one study, and less than SLSF in the remaining nine studies. Average total mean PLSF of 8.27% was significantly greater than the mean SLSF of 3.27% ($p = 0.001$; Table 2). When grouping patients by PLSF ranges of < 10%, 10–19.9%, and ≥ 20%, PLSF was significantly greater

Fig. 1 Patient with hepatitis C cirrhosis and HCC involving segments 2 and 3. a Planar scintigraphy using anterior and posterior views demonstrates a LSF of 25.7%. b SPECT/CT with semiautomated segmentation software demonstrates a LSF of 14.7%. SPECT/CT LSF evaluation allows more accurate organ segmentation and delineation of liver from lung
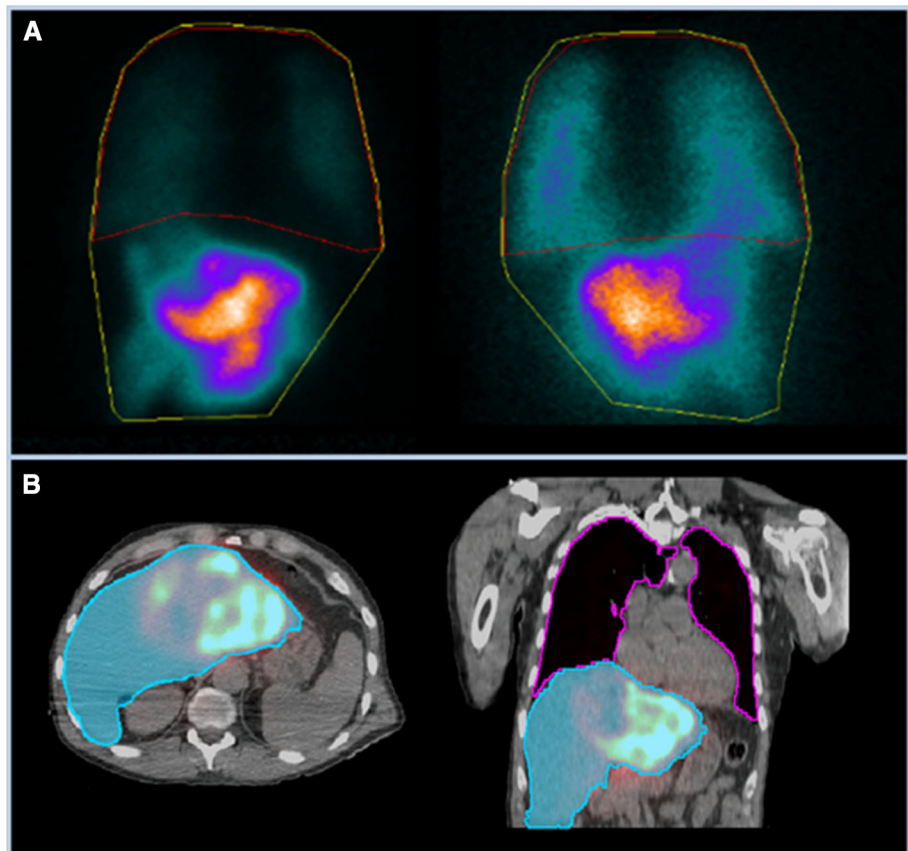
Table 1 Baseline characteristics

Patients (n)	293
Age (years)	64.5
Sex (n)	
Male	231 (78.8%)
Female	62 (21.2%)
Race (n)	
White	173
Black	85
Asian	21
Other/unknown	10
Hispanic	3
Native American	1
Liver cancer etiology (n)[a]	
Hepatitis C	167
Alcohol	61
NASH[b]	36
Idiopathic/unknown	35
Hepatitis B	30
Other/miscellaneous	8
Hemochromatosis	5
BCLC stage (n)	
0, A, or B	184
C	34
Childs–Pugh score (n)	
A	243
B or C	50
Mean PLSF (%)	8.27

[a]Multiple patients had more than one etiology for liver cancer

[b]Nonalcoholic stateohepatitis

than SLSF in all groups, respectively (p's = 0.001; Table 2). After evaluating patients by largest liver lesion size of < 5, 5–10 cm, and ≥ 10 cm, mean PLSF was significantly greater than SLSF in all groups, respectively (p = 0.0001, 0.0001, and 0.0045; Table 2). Mean PLSF remained significantly greater than SLSF when comparing greater/worse BCLC stages and C–P scores (p's = 0.0001; Table 2).

Total mean absolute discrepancy between PLSF and SLSF in all patients was 5.01% (range 5.59–18.57%; Table 3). In patients with a planar LSF of ≥ 20%, the absolute discrepancy was 13.3%. This was significantly greater than patients with a PLSF of < 20%, who had an absolute discrepancy of 4.74% (p = 0.001; Table 3). Absolute discrepancy was greater among patients with a largest liver lesion size of ≥ 5.0 cm compared to patients with a liver lesion size of < 5.0 cm (5.59% vs 4.40%; p = 0.0076; Table 3). The absolute discrepancy was

significantly greater among patients with a C–P score of B/C compared to those with a C–P score of A (6.12% for C–P B/C vs 4.78% for C–P A; p = 0.0081). There was no significant difference in absolute discrepancy among patients with a BCLC stage of 0/A/B versus BCLC stage C (4.87% for 0/A/B vs 4.56% for C; p = 0.5993).

Multiple linear regression analyses were conducted to examine whether discrepancy in PLSF and SLSF was moderated by potential factors (Table 4). When adjusted for age, gender, and race the discrepancy between PLSF and SLSF was significantly greater in patients with a PLSF of ≥ 20% (β = 4.41; 95% CI 2.47, 6.35; p < 0.0001) and a largest lesion size of ≥ 5 cm (β = 0.53; 95% CI: 0.09, 0.97; p = 0.019). Following additional adjustment for liver cancer etiology, a significantly greater discrepancy was observed in patients with a PLSF ≥ 20% (β = 4.68; 95% CI: 2.61, 6.74; p < 0.0001), largest lesion size ≥ 5 cm (β = 0.55; 95% CI: 0.10, 0.98; p = 0.0164), and Child–Pugh Score B/C (β = 2.67; 95% CI: 1.02, 4.32; p = 0.0226). There was no significant effect modification from interactions between covariates on the discrepancy between PLSF and SLSF.

Discussion

Growing evidence indicates that effective Y-90 RE is dependent on appropriate dose calculation, so that sufficient threshold activity is delivered to target tumors [10–13]. For example, Vouche et al. demonstrate that complete pathological necrosis and local tumor control is improved when a dose of > 190 Gy is achieved in patients with HCC undergoing radiation segmentectomy with glass microspheres [10].

Optimal dose calculation is contingent on accurate pre-procedural LSF calculation. Although there is no gold standard to reference in human studies, several phantom studies have attempted to identify the accuracy of SLSF versus PLSF by comparing it to a known LSF [6, 17, 18]. Zaharakis et al. in their phantom study concluded that "SPECT/CT is significantly more accurate than the manufacturer suggested planar method for estimating hepatopulmonary shunts [18]". In a study by Allred et al., for a phantom with a true LSF of 3.6%, PLSF was 5.12%, and SLSF was 3.1% [6]. Another phantom study by Gill et al. found that for a true LSF of 9.9%, PLSF was 18.5%, and SLSF was 9.5% [17].

Human studies have corroborated the phantom studies, showing that PLSF overestimates the true LSF and thus may result in reduced delivered dose [8, 9, 16, 19]. For example, a study by Yu et al. evaluating 71 patients with primary and metastatic hepatic malignancies who underwent Y-90 RE demonstrated that mean lung dose was

Table 2 Mean PLSF versus SLSF

Group (n)	Planar LSF % (SD)[a]	SPECT/CT LSF % (SD)	p value*
Total (293)	8.27 (4.84)	3.27 (2.63)	< 0.0001*
Planar LSF range			
< 10% (221)	6.02 (1.95)	2.34 (1.57)	< 0.0001*
10–19.9% (63)	13.89 (2.65)	5.41 (2.49)	< 0.0001*
≥ 20% (9)	24.29 (4.11)	10.98 (3.23)	< 0.0001*
Liver tumor size (largest lesion)			
< 5.0 cm (141)	7.05 (3.76)	2.64 (2.14)	< 0.0001*
5–10 cm (65)	9.74 (5.72)	4.18 (3.28)	< 0.0001*
≥ 10 cm (12)	10.96 (5.34)	5.17 (3.42)	0.0045*
BCLC stage			
0, A, or B (184)	8.12 (4.82)	3.25 (2.85)	< 0.0001*
C (34)	7.79 (4.13)	3.23 (1.95)	< 0.0001*
Child–Pugh score			
A (243)	7.96 (4.76)	3.18 (2.51)	0.0001*
B or C (50)	9.80 (4.98)	3.68 (3.17)	0.0001*

*$p < 0.05$

[a]SD = standard deviation

Table 3 Absolute discrepancy between PLSF and SLSF

Group (n)	% Discrepancy between PLSF and SLSF (SD)[a]	p value*
Planar LSF range		
< 20% (284)	4.74% (2.89)	
≥ 20% (9)	13.3% (4.27)	0.0001*
Liver tumor size		
< 5 cm (141)	4.40 (2.74)	
≥ 5 cm (77)	5.59 (3.71)	0.0076*
BCLC stage		
0, A, or B (184)	4.87 (3.12)	
C or D (34)	4.56 (3.22)	0.5993
Child–Pugh score		
A (243)	4.78 (3.33)	
B or C (50)	6.12 (2.78)	0.0081*

*$p < 0.05$

[a]SD = standard deviation

Table 4 Discrepancy between PLSF and SLSF predicted by linear regression models[a]

Covariates	Discrepancy between planar and SPECT/CT LSF			
	Model 1 β (95% CI)	p value*	Model 2 β (95% CI)	p value*
Planar LSF (< 20% vs ≥ 20%)	4.41 (2.47, 6.35)	< 0.0001*	4.76 (2.66, 6.85)	< 0.0001*
Largest lesion size (< 5 cm vs ≥ 5 cm)	0.53 (0.09, 0.97)	0.0190*	0.66 (0.19, 1.13)	0.0066*
BCLC stage (0, A, or B vs C)	0.94 (− 0.93, 2.92)	0.3233	0.94 (− 1.10, 2.99)	0.3634
Child–Pugh score (A vs B or C)	0.70 (− 0.84, 2.23)	0.3701	2.62 (0.31, 4.92)	0.0265*

[a] Model 1 was adjusted for age, gender and race. Model 2 was additionally adjusted for liver cancer etiology and number of primary cancers

*$p < 0.05$

overestimated with planar scintigraphy when compared with SPECT/CT [16]. This effect was more profound in patients with a higher mean lung dose calculated by planar scintigraphy (> 15 Gy), where the mean overestimation with planar scintigraphy compared to SPECT/CT was 170% [16]. This is corroborated by Dittman et al., who prospectively analyzed 50 consecutive patients with primary and metastatic hepatic malignancies revealing that SLSF was lower in all patients, with a mean of just 1.9% (range 0.8–15.7%), compared to 6.8% (range 3.4–32.3%) with PLSF [8]. They also reported ten patients (20%) who had a LSF of greater than 10% using planar scintigraphy, which may result in dose adjustments or contraindications to Y-90 RE. This is contrasted to just two patients (4%) with greater than 10% LSF using SPECT/CT [8].

This large series retrospective analysis is concordant with prior studies, demonstrating that PLSF is greater than SLSF in the majority of patients with HCC. In fact, only nine of 293 (3.1%) patients had a PLSF less than SLSF. While it is not entirely clear why PLSF was less than SLSF in these patients, it is notable that these patients had Tc-99m MAA activity near the hepatic dome. It may be that ROI boxes drawn over the region of the liver on planar imaging were oversized and included a large portion of the lung bases, resulting in a falsely low PLSF. Such findings may also be related to statistical variation.

This study expands on prior studies by demonstrating that PLSF remained greater than SLSF regardless of multiple baseline factors including PLSF range, maximum liver lesion size, BCLC stage, and C–P score. As seen in the study by Yu et al., the discrepancy with SLSF was even more profound in patients with greater PLSF. In our series, absolute discrepancy between PLSF and SLSF was significantly greater among patients with a PLSF of ≥ 20%. A greater discrepancy was also identified in patients with a greater maximum liver lesion size and C–P score (but not BCLC stage). In our series, baseline PLSF was greater among patients with these features. Thus, in patients with a larger PLSF, differences between PLSF and SLSF may be exaggerated. Such findings iterate the importance of accurate LSF assessment, as patients with elevated LSF may receive significant dose reductions or be deemed ineligible for Y-90 RE. Furthermore, evidence indicates that elevated LSF, larger tumors, and worse liver function are associated with more aggressive malignancies [20–23]. This may necessitate repeat Y-90 RE, which requires an even greater emphasis on accurate dose calculation in order to optimize therapy without exceeding cumulative liver or lung dose limits. More analyses would be necessary to validate these inferences.

This study is limited by its retrospective nature. Five patients were excluded from the analysis due to incomplete acquisition of the upper thorax on SPECT/CT images, which may have skewed results. Another limitation was that this study only included patients with HCC, who on average have greater LSF than patients with other hepatic malignancies [24, 25]. The differences in LSF between planar scintigraphy and SPECT/CT may differ in patients with other hepatic malignancies. Finally, inter-rater reliability for SLSF was not assessed, so there may be discrepancies in results based on the operator performing manual modifications. Despite these limitations, this relatively large series confirms that estimated hepatopulmonary shunting is greater when measured with planar imaging, and that discrepancies between PLSF and SLSF are greater in patients with HCC who have greater PLSF, larger tumors, and worse baseline C–P score. Future prospective studies analyzing potential differences in delivered dose would be useful to analyze whether the use of SPECT/CT can minimize non-tumoral dose and improve Y-90 treatment response. Given that using SLSF in treatment planning might allow opportunities to optimize dose and increase eligibility for patients to undergo Y-90, we believe it would be prudent to consider adopting this method with close radiation safety monitoring.

Conclusion

In patients with HCC, Tc-99m MAA LSF calculated with SPECT/CT appears to be significantly lower compared to planar imaging, with a greater discrepancy among patients with a PLSF fraction of greater than 20%, tumor size ≥ 5 cm, and worse CP score.

References

1. Camacho JC, Moncayo V, Kokabi N, Reavey HE, Galt JR, Yamada K, et al. 90Y radioembolization: multimodality imaging pattern approach with angiographic correlation for optimized

target therapy delivery. RadioGraphics. 2015;35(5):1602–18. https://doi.org/10.1148/rg.2015140314.

2. Bhangoo MS, Karnani DR, Hein PN, Giap H, Knowles H, Issa C, et al. Radioembolization with Yttrium-90 microspheres for patients with unresectable hepatocellular carcinoma. J Gastrointest Oncol. 2015;6(5):469–78. https://doi.org/10.3978/j.issn.2078-6891.2015.056.

3. Gordon AC, Gabr A, Riaz A, Uddin OM, Abouchaleh N, Ali R, et al. Radioembolization super survivors: extended survival in non-operative hepatocellular carcinoma. Cardiovasc Intervent Radiol. 2018;41(10):1557–655. https://doi.org/10.1007/s00270-018-2008-y.

4. Wehrenberg-Klee E, Gandhi RT, Ganguli S. Patient selection and clinical outcomes of Y90 in hepatocellular carcinoma. Tech Vasc Intervent Radiol. 2019;22(2):70–3. https://doi.org/10.1053/j.tvir.2019.02.006.

5. Kooby DA, Egnatashvili V, Srinivasan S, Chamsuddin A, Delman KA, Kauh J, et al. Comparison of yttrium-90 radioembolization and transcatheter arterial chemoembolization for the treatment of unresectable hepatocellular carcinoma. JVIR. 2010;21(2):224–30. https://doi.org/10.1016/j.jvir.2009.10.013.

6. Allred JD, Niedbala J, Mikell JK, Owen D, Frey KA, Dewaraja YK. The value of (99m)Tc-MAA SPECT/CT for lung shunt estimation in (90)Y radioembolization: a phantom and patient study. EJNMMI Res. 2018;8(1):50. https://doi.org/10.1186/s13550-018-0402-8.

7. Leung WT, Lau WY, Ho SK, Chan M, Leung NW, Lin J, et al. Measuring lung shunting in hepatocellular carcinoma with intrahepatic-arterial technetium-99m macroaggregated albumin. J Nuclear Med. 1994;35(1):70–3.

8. Dittmann H, Kopp D, Kupferschlaeger J, Feil D, Groezinger G, Syha R, et al. A prospective study of quantitative SPECT/CT for evaluation of lung shunt fraction before SIRT of liver tumors. J Nuclear Med. 2018;59(9):1366–72. https://doi.org/10.2967/jnumed.117.205203.

9. Kao YH, Magsombol BM, Toh Y, Tay KH, Chow PK, Goh AS, et al. Personalized predictive lung dosimetry by technetium-99m macroaggregated albumin SPECT/CT for yttrium-90 radioembolization. EJNMMI Res. 2014;4:33. https://doi.org/10.1186/s13550-014-0033-7.

10. Vouche M, Habib A, Ward TJ, Kim E, Kulik L, Ganger D, et al. Unresectable solitary hepatocellular carcinoma not amenable to radiofrequency ablation: multicenter radiology-pathology correlation and survival of radiation segmentectomy. Hepatology (Baltimore, MD). 2014;60(1):192–201. https://doi.org/10.1002/hep.27057.

11. Strigari L, Sciuto R, Rea S, Carpanese L, Pizzi G, Soriani A, et al. Efficacy and toxicity related to treatment of hepatocellular carcinoma with 90Y-SIR spheres: radiobiologic considerations. J Nuclear Med. 2010;51(9):1377–85. https://doi.org/10.2967/jnumed.110.075861.

12. Srinivas SM, Natarajan N, Kuroiwa J, Gallagher S, Nasr E, Shah SN, et al. Determination of radiation absorbed dose to primary liver tumors and normal liver tissue using post-radioembolization (90)Y PET. Front Oncol. 2014;4:255. https://doi.org/10.3389/fonc.2014.00255.

13. Demirelli S, Erkilic M, Oner AO, Budak ES, Gunduz S, Ozgur O, et al. Evaluation of factors affecting tumor response and survival in patients with primary and metastatic liver cancer treated with microspheres. Nucl Med Commun. 2015;36(4):340–9. https://doi.org/10.1097/mnm.0000000000000257.

14. Kennedy A, Nag S, Salem R, Murthy R, McEwan AJ, Nutting C, et al. Recommendations for radioembolization of hepatic malignancies using yttrium-90 microsphere brachytherapy: a consensus panel report from the radioembolization brachytherapy oncology consortium. Int J Radiat Oncol Biol Phys. 2007;68(1):13–23. https://doi.org/10.1016/j.ijrobp.2006.11.060.

15. Sarfaraz M, Kennedy AS, Lodge MA, Li XA, Wu X, Yu CX. Radiation absorbed dose distribution in a patient treated with yttrium-90 microspheres for hepatocellular carcinoma. Med Phys. 2004;31(9):2449–533. https://doi.org/10.1118/1.1781332.

16. Yu N, Srinivas SM, Difilippo FP, Shrikanthan S, Levitin A, McLennan G, et al. Lung dose calculation with SPECT/CT for (9)(0)Yittrium radioembolization of liver cancer. Int J Radiat Oncol Biol Phys. 2013;85(3):834–9. https://doi.org/10.1016/j.ijrobp.2012.06.051.

17. Gill H, Bian J, Gabriel M, Molvar C, Wagner R, Halama J. 99mTc-MAA SPECT/CT imaging for quantitative assessment of lung shunt fraction prior to 90Y transarterial radioembolization. J Nuclear Med. 2019;60(supplement 1):265.

18. Zaharakis A, Leveque F, Backiel J, Tursi G, Palestro C, Nichols K. SPECT/CT for estimating hepatopulmonary shunting in selective internal radiotherapy: a phantom study. J Nucl Med. 2014;55(supplement 1):1496.

19. Elschot M, Nijsen JF, Lam MG, Smits ML, Prince JF, Viergever MA, et al. ((9)(9)m)Tc-MAA overestimates the absorbed dose to the lungs in radioembolization: a quantitative evaluation in patients treated with (1)(6)(6)Ho-microspheres. Eur J Nuclear Med Mol Imaging. 2014;41(10):1965–75. https://doi.org/10.1007/s00259-014-2784-9.

20. Deipolyi AR, Iafrate AJ, Zhu AX, Ergul EA, Ganguli S, Oklu R. High lung shunt fraction in colorectal liver tumors is associated with distant metastasis and decreased survival. JVIR. 2014;25(10):1604–8. https://doi.org/10.1016/j.jvir.2014.06.019.

21. Ludwig JM, Ambinder EM, Ghodadra A, Xing M, Prajapati HJ, Kim HS. Lung shunt fraction prior to yttrium-90 radioembolization predicts survival in patients with neuroendocrine liver metastases: single-center prospective analysis. Cardiovasc Intervent Radiol. 2016;39(7):1007–144. https://doi.org/10.1007/s00270-016-1323-4.

22. Dendy MS, Ludwig JM, Kim HS. Predictors and prognosticators for survival with Yttrium-90 radioembolization therapy for unresectable colorectal cancer liver metastasis. Oncotarget. 2017;8(23):37912–22. https://doi.org/10.18632/oncotarget.16007.

23. Antkowiak M, Gabr A, Das A, Ali R, Kulik L, Ganger D, et al. Prognostic role of albumin, bilirubin, and ALBI scores: analysis of 1000 patients with hepatocellular carcinoma undergoing radioembolization. Cancers (Basel). 2019;11(6):879. https://doi.org/10.3390/cancers11060879.

24. Elsayed M, Martin JG, Dabrowiecki A, Goldman DT, Faraj R, McMahon JT, et al. Tc-99m-MAA lung shunt fraction before Y-90 radioembolization is low among patients with non-hepatocellular carcinoma malignancies. Nucl Med Commun. 2019; 40(11):1154–7. https://doi.org/10.1097/mnm.0000000000001089.

25. Gaba RC, Zivin SP, Dikopf MS, Parvinian A, Casadaban LC, Lu Y, et al. Characteristics of primary and secondary hepatic malignancies associated with hepatopulmonary shunting. Radiology. 2014;271(2):602–12. https://doi.org/10.1148/radiol.14131969.